

1  
2  
3  
4  
5  
6  
7  
8  
9  
10  
11  
12  
13  
14  
15  
16  
17  
18  
19  
20  
21  
22  
23

## **REVISION 2**

# ***The rapid expansion of environmental mineralogy in unconventional ways: Beyond the accepted definition of a mineral, the latest technology, and using nature as our guide***

Manuel A. Caraballo<sup>1,2,3\*</sup>, F. Marc Michel<sup>1</sup> and Michael F. Hochella, Jr.<sup>1</sup>

<sup>1</sup> *Department of Geosciences, Virginia Tech, Blacksburg, Virginia 24061, U.S.A.*

<sup>2</sup> *Geology Department, University of Huelva, Campus "El Carmen", E-21071 Huelva, Spain*

<sup>3</sup> *Mining Engineering Department, University of Chile, Avda. Tupper 2069 Santiago, Chile*

---

\* Corresponding author. Tel.: +34-667568619

E-mail address: [macaraballomonge@gmail.com](mailto:macaraballomonge@gmail.com) (Manuel A. Caraballo)

24

25

## ABSTRACT

26 Environmental mineralogy is rapidly expanding in technological directions that allow for the  
27 detection, characterization, and understanding of non-crystalline and poorly crystalline  
28 phases, crystalline-amorphous mixed phases, and nanosized naturally-occurring materials.  
29 Specifically, this article provides a perspective view of the broad range of structural  
30 complexity/heterogeneity observed in environmental minerals and amorphous materials, as  
31 well as our current understanding of how these materials can be best observed, evaluated, and  
32 described, and why this is important in the mineralogical sciences. The discussion is broken  
33 down into the assessment of short- and medium-range order in amorphous materials, and the  
34 nature of nanominerals and mineral nanoparticles, amorphous-nanocrystalline transitional  
35 phases, and mesocrystals. These materials do not fit one or more aspects of the most  
36 commonly used definitions of a mineral (although some of them are formally recognized as  
37 minerals, such as ferrihydrite and schwertmannite), yet they do fit other portions of these  
38 current definitions. Nevertheless, because these phases can be exceptionally minute in size,  
39 and/or not highly crystalline, and/or generally much less abundant than other mineral  
40 components in the system, they may be underappreciated and/or understudied, or, apparently  
41 as is often the case, completely missed. Yet they are often highly relevant to, and in many  
42 cases dominant in, important aspects of how the (bio)geochemistry of an environmental  
43 system operates. Further, although it is important to analytically and experimentally  
44 characterize synthetic equivalent phases in the laboratory, often under conditions intended to  
45 mimic one or a few aspects of the real environment, we argue that it is imperative to study  
46 natural, intact (as much as possible) samples and make field measurements with much greater  
47 frequency than is currently practiced.

48

49

50

## KEYWORDS

51 Environmental mineralogy, synchrotron radiation, free electron laser, transmission electron  
52 microscopy, nanomineral, mineral nanoparticle, polyphasic nanomineral, prenucleation  
53 cluster, non-classical crystallization, mesocrystal.

54

55

56

## INTRODUCTION

57

58

59

60

61

62

63

It is very well known, especially among mineralogists, geochemists, and geophysicists, that knowledge of atomic structure has proven crucial time and again in understanding mineral behavior including: compressibility, elasticity, thermal behavior, density, hardness, optical properties, solubility, adsorption and desorption tendencies, transformation characteristics, thermodynamic properties, etc. Indeed, the accessibility of such information through mineralogy has had tremendous implications for our understanding of geological and environmental processes on Earth as well as on other planets.

64

65

66

67

68

69

70

71

72

73

74

75

76

77

78

79

80

81

82

83

84

85

86

Yet despite the obvious importance of atomic structure and the central role that it plays, it has become more apparent over the years that crystallinity is the most difficult aspect to measure and describe, especially when the periodicity of the structure is reduced. Further, as we point to throughout this paper, this can be viewed as having fundamental consequences in terms of being able to express a precise definition of a mineral. A classic and still widely-accepted definition of a mineral can be stated as follows: a solid formed as a result of a geological process and characterized by a periodic array of atoms with a known structure, definite chemical composition, and discrete (indexable) diffraction signature (Nickel 1995; International Union of Crystallography, Report of the Executive Committee for 1991). Nevertheless, especially over the last 20 years, the reported definitions of a mineral, as stated in introductory geoscience- and mineralogy-related textbooks and on-line, generally have become progressively broader and more detailed. To some extent, this is likely due to advancement of the mineralogical sciences that is, in part, driven by new characterization tools and methods, and also by an expansion of the types of scientists who are interested in minerals. Recently, French et al. (2012) compiled up-to-date, authoritative descriptions of the term mineral, producing the following definition: “Currently, minerals are most commonly defined as naturally occurring substances, produced by (bio)geochemical processes, with a highly ordered, repeating atomic arrangement (a crystalline substance) whose composition can be described by a chemical formula that is either fixed or variable (or, also as often stated, a definite, but not necessarily fixed, composition). Samples of the same mineral vary in terms of minor and/or trace element composition, and in the case of solid solution, major element composition, as long as these substitutions do not change the average crystal structure. Finally, it follows that minerals of the same major and minor

87 element composition will express a set of measurable and consistent physical and chemical  
88 properties.” Even this definition can be reasonably challenged and/or debated in various  
89 places (e.g., among many others, Klein and Dutrow, 2008; Hochella et al., 2008; Bindi et al.,  
90 2011; Bindi and Steinhardt, 2012; French et al., 2012).

91       Whatever the exact definition of mineral that one uses, such descriptive elements are  
92 broadly applicable to what we observe in vast assemblages of fundamental Earth materials  
93 that comprise the igneous, sedimentary, and metamorphic rocks in Earth’s crust, as well as  
94 the thin veneer (relatively speaking) of soil and aqueous environments encompassing Earth’s  
95 near-surface. In this regard, crystallinity has always been quintessential in terms of what  
96 defines a mineral because three-dimensional periodicity (except in quasicrystals) is what  
97 makes the average atomic structure accessible by modern diffraction methods. The Rietveld  
98 method (Rietveld, 1969) of analyzing single crystal and powder diffraction data in  
99 reciprocal-space has long been the standard for determining long-range structure in  
100 crystalline materials. Indeed, modern Bragg diffraction and crystallographic methods have  
101 revealed the average crystal structures of several thousand minerals to date, not to mention  
102 several hundred thousand organic, organo-metallic, and inorganic compounds, and metals  
103 and alloys that are not naturally-occurring.

104       Although crystallinity is abundant in Earth materials, it is important to bear in mind  
105 that crystals produced in nature (and laboratory) are not flawless at the atomic level. Local  
106 atomic displacements away from the average long-range structure are present even in the  
107 most highly crystalline materials due to occurrences of point (e.g., vacancies or substitutions  
108 of atoms), linear (dislocations), and planar (grain boundaries, stacking faults, external  
109 surfaces) defects. Imperfections in gem-quality natural diamonds, for example, often are the  
110 result of vacancies, dislocations, and atomic inclusions of impurities e.g., nitrogen or boron.  
111 In the case of diamond, as well as for numerous other minerals, defects and lattice relaxation  
112 around the defects (e.g., strain) are extremely important due to the considerable impacts they  
113 have on optical, physical, chemical, or mechanical properties. In addition to internal  
114 structural defects in crystals, we also now know that the arrangements of atoms at and near  
115 the surfaces can differ substantially from their bulk equilibrium positions, and normally are  
116 not fully represented by models based on ideal surface terminations of the bulk structure.  
117 The phenomenon of surface relaxation and reconstruction, which includes modifications in  
118 periodicity, symmetry changes, and an overall increase in structural disorder in the first few  
119 atomic layers near the surface of the crystal, is inevitable as the system strives to reduce



152 X-rays in 1895 by Wilhelm Conrad Röntgen and its later application to the study of mineral  
153 crystal structures, by means of the X-ray diffraction phenomena and Bragg's law (Bragg,  
154 1912), has been the most important technical revolution in this field. Since then, some other  
155 very important techniques have been incorporated into the study of mineral crystallinity such  
156 as electron and neutron diffraction, nuclear magnetic resonance (NMR), and infrared and  
157 Raman spectroscopy, among others (Fig. 1A). Although not suitable for determining  
158 structure directly, it is also noteworthy that optical mineralogical methods and use of the  
159 polarizing light microscope has contributed immensely to our knowledge of minerals and  
160 rocks.

161         However, a second technological revolution, during the last 20 years, is launching the  
162 fields of mineral crystallinity and environmental mineralogy to an entirely new dimension.  
163 This new era mainly relies on the discoveries and innovations achieved in both synchrotron  
164 light sources and transmission electron microscopy (TEM).

165         Synchrotrons generate intense radiation (from the infrared to 'hard' X-rays in the  
166 electromagnetic spectrum, Fig.1 B) and typically display high brilliance, tunability, low  
167 divergence and low emittance of the beam. The first dedicated parasitic synchrotron light  
168 sources were developed in the mid-1970s. Since that time, new generations of synchrotrons  
169 have progressively become optimized for high brilliance (or brightness). Peak brilliance (PB  
170 = photon flux per unit transverse and longitudinal phase-space volume, photons/sec mrad<sup>2</sup>  
171 mm<sup>2</sup> 0.1%BW) in the current "3<sup>rd</sup> generation" synchrotron radiation facilities has increased  
172 more than nine orders of magnitude (10<sup>19</sup> to 10<sup>25</sup> PB, Fig. 1B) compared to conventional X-  
173 ray sealed tubes (10<sup>8</sup> to 10<sup>10</sup> PB), allowing the appearance or enhancement of a variety of X-  
174 ray techniques. In general, this is because cyclic accelerators are uniquely equipped with  
175 insertion devices that alter the properties of the X-ray beam. These devices typically include  
176 wigglers, which provide continuous energy spectrums, and undulators, which operate at  
177 discrete energies but deliver extremely high flux. Other devices used for conditioning the  
178 characteristics (specific energy, dimensions, etc.) of the radiation beam include  
179 monochromators, mirror optics, collimators and slits, among others. These elements are  
180 typically combined with state-of-the art 1-D and 2-D detector systems having high spatial  
181 and/or energy resolution that measure the radiation that has interacted with the sample.  
182 Overall, synchrotron beamlines are typically equipped for spectroscopy, scattering, and/or  
183 imaging experiments and the facilities are designed to accommodate a broad range of studies  
184 involving chemistry, physics, biology, and materials sciences.

185 Modern synchrotrons support a wide variety of methods and experiments that are well  
186 suited for the earth sciences, including studies of mineral crystal chemistry and mineral  
187 behavior in complex earth material matrices. The unique properties of synchrotron light, in  
188 particular the brightness and tunability, has permitted the growth of many X-ray scattering  
189 based techniques such as X-ray total scattering and pair distribution function (PDF), small  
190 angle X-ray scattering (SAXS), surface X-ray scattering methods such as crystal truncation  
191 rod (CRT) diffraction, photoelectron scattering (X-ray absorption fine structure, XAFS), and  
192 grazing incidence methods (e.g., long-period X-ray standing wave, LP-XSW). Synchrotron  
193 light has also enhanced some well established techniques (e.g.,  $\mu$ -XRD and  $\mu$ -XRF) which  
194 have gained spatial resolutions down to 100 nm. These methods open up the possibility of  
195 studying characteristics of minerals with sensitivities and at resolutions that are normally not  
196 achievable with laboratory X-ray sources. Static experiments of single crystal and  
197 polycrystalline samples at ambient conditions are common, and include studies of bulk  
198 structures and the nature of defects and disorder in natural materials ranging from crystalline  
199 to amorphous. In addition, many of the aforementioned techniques allow studies of minerals  
200 in situ under a wide variety of conditions ranging from water at environmental conditions  
201 (Majzlan and Myneni, 2005) to melts or solids at high P-T conditions (e.g., 73GPa and  
202 1700K; Lin et al., 2005). For additional information on synchrotrons and the use of  
203 synchrotron radiation in the study of Earth materials, the reader is referred to the *Elements*  
204 issue entitled “User research facilities in the Earth Sciences” (Sutton, 2006) and articles  
205 therein.

206 Although the trend of increasing brightness in synchrotrons over the last 30 years has  
207 been impressive, the limits are now being pushed even further by the new generation of free-  
208 electron lasers (FEL) that, just in the last five years, have been able to achieve peak  
209 brilliances ( $10^{29}$  to  $10^{34}$  PB) nine orders of magnitude higher than the current 3<sup>rd</sup> generation  
210 synchrotrons (Fig. 1B). In addition to this outstanding peak brilliance, FELs typically display  
211 ultrashort pulse durations of about 100fs (at least 100 times shorter than common  
212 synchrotrons), and 7fs pulses have been demonstrated using the Linac Coherent Light Source  
213 (LCLS) at Stanford University, USA. These unprecedented conditions are paving the way to  
214 explore new fields in mineralogy like femtosecond nanocrystallography and coherent X-ray  
215 imaging with nanometer resolution as recently demonstrated with a pioneering study of soot  
216 particles in flight (Loh et al., 2012). For additional information and perspectives in FELs, the  
217 reader is referred to Ullrich et al. (2012).

218 Transmission electron microscopy is the other essential pillar supporting many of the  
219 new discoveries in mineral crystallinity and environmental mineralogy. Since the first TEM  
220 was built by Max Knoll and Ernst Ruska in 1931, imaging resolution has improved by nearly  
221 three orders of magnitude, starting at roughly 10 nm (Fig. 1C) for the first commercial  
222 instruments in the late 1930's (Rickerby et al., 1999), to atomic resolution (0.045 nm)  
223 achieved by the current aberration-corrected high resolution-TEMs (Barton et al., 2012). In  
224 addition to atomic scale imaging, the interactions between an electron beam and the  
225 constituent atoms of a sample also generate a wealth of information that can be interpreted by  
226 the use of various powerful analytical techniques such as electron diffraction (ED; often  
227 essential for phase identification, but also used for a wide variety of crystallographic studies)  
228 and selected area electron diffraction (SAED; ED from areas ranging from microns to 5-10  
229 nanometers in diameter); energy-dispersive X-ray spectroscopy (EDS; chemical analysis  
230 with spatial resolution down to single atomic columns, now using exceptionally efficient  
231 large area silicon drift detectors); energy filtered TEM (EFTEM, imaging formed from  
232 electrons of a particular energy only); electron energy loss spectroscopy, especially when  
233 combined with EFTEM imaging (EELS); electronic structure and bonding studies; electron  
234 tomography (3-D images of any object in a TEM specimen); high angle annular dark field  
235 scanning TEM (HAADF-STEM; image contrast as a result of average atomic number at  
236 every position of the highly focused scanning beam, and also used for tomographic images);  
237 and high resolution TEM (HR-TEM; lattice fringe imaging, with corresponding fast Fourier  
238 transform – FFT – images). All of these imaging, analytic, and crystallographic capabilities  
239 place electron microscopy as possibly the single most versatile technique in mineralogy  
240 today.

241 These exceptional advances in electron microscopy are leading to new studies almost  
242 unthinkable just a decade ago, such as highly detailed three dimensional imaging of  
243 nanoparticles, and dynamic observations of the physical behavior of nanoparticles in aqueous  
244 solutions. Concerning the former, some of the unique attributes of nanominerals arise from  
245 three-dimensional (3D) spatial features. In principle, electron tomographic reconstructions  
246 use algorithms to infer 3D geometry from a series of conventional 2D projections taken from  
247 different perspectives. It has been shown recently that 3D reconstructions give more accurate  
248 nanoparticle size and spacing information than conventional 2D imaging (Monsegue et al., in  
249 press). At atomic resolution, it is much more challenging to achieve electron tomographic  
250 reconstructions because the 2D micrographs must be aligned with a spatial accuracy better



251 than the imaged interatomic spacing. Nevertheless, several electron tomography strategies  
252 have been developed to achieve reconstructions with full atomic-scale resolution (Van Aert  
253 et al., 2011; Van Dyck et al., 2012; Scott et al., 2012). There are practical challenges to  
254 implementing these strategies, however, including difficulty tilting a sample through large  
255 angles with enough mechanical precision to permit atomic resolution reconstruction, and the  
256 need to rely on an assumed structure model to infer atom positions along the electron beam  
257 direction. A model-free strategy was recently demonstrated (Scott et al., 2012), but accurate  
258 image alignment remains a barrier to reconstructing arbitrary/defective nanostructured  
259 crystals with atomic resolution.

260 Finally, recent advances in *in situ* TEM offers dynamic observations of the physical  
261 and chemical behavior of nanominerals in response to external parameters including  
262 temperature, atmosphere, stress, solutions, etc; that may be far from equilibrium conditions  
263 (if desired) in relatively short to moderate periods of time (hours to days). After many  
264 decades of hardware development, reliable environmental cell construction for examining  
265 solid-gas, solid-solid and liquid-solid phase interactions are now commercially available,  
266 allowing for imaging at sub-nanometer resolution levels (see, e.g., Woehl et al., 2013). For  
267 nanoparticles, particularly important recent advances include the observation of oriented  
268 attachment of nanominerals in aqueous solution and in real time (Li et al., 2012), and  
269 nanocrystalline growth in aqueous solution viewed with atomic resolution in real time (Yuk  
270 et al., 2012). These types of studies show phenomena that have never been observed and/or  
271 predicted before, and therefore are revolutionary in advancing science.

272 Comprehensive information about transmission electron microscopy and associated  
273 techniques can be found in the compendium by Williams and Carter (2009).

274 As shown in Figure 1A, it is worth noting that each of the many analytical techniques  
275 available to study mineral crystallinity has a specific “high efficiency” limited range.  
276 Consequently, it is essential to realize that the current revolution in the study of mineral  
277 crystallinity and environmental mineralogy is, and will be, possible not only because of the  
278 advances in a few analytical techniques, but mainly because of the synergistic interaction  
279 among the many techniques covering different scales and analytical approaches.

280 **EMERGING AREAS IN THE FIELD OF MINERAL CRYSTALLINITY FOR**  
281 **ENVIRONMENTAL SYSTEMS**

282 For the sake of clarity and to facilitate the discussion in the following sections, the  
283 natural progressive transition between amorphous and crystalline materials will be  
284 categorized according to material periodicity and size (Fig. 2). Material periodicity can be  
285 understood as the nature of regularly appearing recurrent motifs as one moves through an  
286 atomic structure, and it is convenient to compartmentalize this regularity in terms of short-,  
287 medium- and long-range order. The structure of a crystal is composed of a unit cell that  
288 repeats by translational symmetry. As such, long-range order (LRO) is referenced to the  
289 translation from one site to another identical site in a different unit cell in a crystal structure.  
290 Short-range order (SRO), on the other hand, is referenced to a single atom or point in a  
291 structure versus some nearby neighboring atom or shell of atoms. Medium-range order  
292 (MRO), a term that is more often used in literature pertaining to glasses and liquids, is simply  
293 an extension of SRO (e.g., third, fourth, etc. coordination shells). Figure 2 presents these  
294 brief definitions of SRO, MRO, and LRO in terms of interatomic distances. As shown, SRO  
295 is typically limited to periodicity that extends to the third nearest atomic neighbor (distances  
296 generally on the order of up to 0.5 to 0.6 nm), MRO extends periodicity from the fourth to  
297 the tenth nearest neighbor (up to 2 to 3 nm, depending on bond lengths), and finally LRO  
298 accounts for periodicity beyond the tenth nearest neighbor (Lucovsky, 1987). In accordance  
299 with the possible scientific fields defined by this categorization (Fig. 2), the following  
300 emerging areas in material periodicity/crystallinity in environmental systems will be  
301 discussed: SRO and MRO in amorphous materials, nanominerals and mineral nanoparticles,  
302 amorphous-nanocrystalline transitional phases, and mesocrystals.

303 **Short- and medium-range order in amorphous materials**

304 As in the case of crystalline materials, having the correct structural model of an  
305 amorphous solid is important in order to understand its physical-chemical characteristics and  
306 behavior in both natural and materials science settings. Characterizing the structures of  
307 amorphous materials is challenging, however, due to the absence of the sharp Bragg spots or  
308 lines that arise from lattice periodicity (*i.e.*, LRO) in crystalline materials. In materials  
309 lacking LRO, methods for evaluating structure, and the models derived from these methods,  
310 focus on describing the structural ordering over short- and medium-range length scales. For  
311 SRO within compounds, such as a silicate glass, the arrangements of atoms in this region  
312 define the coordination polyhedra, as well as the basic connectivity of these units in a

313 structure. MRO describes correlations between pairs of atoms that occur from the linkages  
314 between coordination polyhedra at greater distances, which in some amorphous structures  
315 can reach a few nanometers (Wright, 1998). Recent studies have shown that our ability to  
316 quantify the short- and medium-range structure of amorphous materials continues to improve  
317 due to advances in both experimental approaches and in structural analysis using  
318 computational methods.

319         The atomic pair distribution function (PDF) technique has been one essential tool in  
320 the development of our understanding of structure in solids that range from exclusively short-  
321 range ordered (i.e., amorphous/glassy) to crystalline with some disorder, as well as in  
322 materials that can be thought of as existing between crystals and glasses (nanocrystalline,  
323 nanoscale and poorly crystallized, paracrystalline, polyphasic, etc.). The PDF is the Fourier  
324 transform of the scattered intensity and describes the real-space distribution of interatomic  
325 distances in a sample. Unlike Bragg diffraction and crystallographic methods that focus on  
326 the occurrences of sharp peaks, the PDF approach does not rely on the presence of LRO.  
327 This is important since a significant proportion of the total integrated intensity resides in the  
328 diffuse scattering in cases of substances that are nanoscale, partially crystallized, and/or  
329 completely disordered. Although the diffuse intensity is relatively weak compared with  
330 Bragg intensity, and is also widely spread over reciprocal space, it contains important  
331 information regarding the SRO and MRO in a sample. A total scattering experiment, from  
332 which the PDF is calculated, measures both the Bragg and diffuse scattering and treats these  
333 on an equal basis. As a result, the method is capable of revealing average structure in  
334 materials that range from crystalline to highly disordered, and virtually everything in  
335 between.

336         From the first study by Debye in 1915 (Debye, 1915) up until the mid-1980s, X-rays  
337 were routinely used in PDF studies because of the availability of laboratory sources. Work  
338 focusing on liquids and amorphous solids during this period resulted in remarkable advances  
339 in our understanding of structure in silica glass, liquid water, and liquid mercury, just to  
340 name a few (see Billinge, 2004, and articles therein for additional information on early works  
341 and the history of PDF). Since the early pioneering works, a great many diffraction studies  
342 of amorphous solid (and liquid) samples have been carried out (see Klug and Alexander,  
343 1974; Warren, 1990; Wright, 1998). Although PDF studies using laboratory X-ray sources  
344 continue, a number of recent studies of amorphous solids have taken advantage of the intense  
345 sources of radiation that are available at 3<sup>rd</sup> generation synchrotron sources. Some of these

346 have involved studies of natural or synthetic analogues of amorphous solids including  
347 carbonates (e.g., Michel et al., 2008, Goodwin et al., 2010; Radha et al., 2012; Reeder et al.,  
348 2013), and silicates (e.g., Poulsen et al., 1995). One benefit of synchrotron radiation is that  
349 high energies (up to 100 keV) allow access to significantly higher scattering angles (or  
350 momentum transfer,  $Q$ ) than is available for most conventional lab sources (e.g., those  
351 equipped with Cu or Mo anode materials). The result is a PDF with higher resolution and  
352 lower termination errors, which are artifacts related to the finite range of scattering data that  
353 is included in the Fourier transform. The extraordinary brilliance of synchrotron X-rays  
354 provides an additional benefit that allows the rapid and accurate measurement of diffuse  
355 intensity, which dominates in amorphous materials, but can be up to 8 orders of magnitude  
356 less than the Bragg intensity observed for polycrystalline samples.

357         Comprehensive information about total scattering and PDF analysis methods can be  
358 found in Egami and Billinge (2003). It is noteworthy that neutrons are used in place of X-  
359 rays in some total scattering/PDF experiments, and can offer distinct advantages depending  
360 on the elements involved (Proffen 2006). For additional information on the use of neutron  
361 scattering in mineral sciences, the reader is referred to Dove (2002) and articles therein.

362         Synchrotron X-ray absorption spectroscopy is a technique that has also greatly added  
363 to our understanding of local atomic structure in amorphous solids. The origins of XAS date  
364 back to the 1920's and 30's (for review see Lytle, 1999). Modern XAS measurements are  
365 typically done using synchrotron X-ray sources since they are able to provide a continuous  
366 and intense X-ray source covering a broad range of energies. XAS data are obtained by  
367 monitoring the interaction of X-rays with a sample as the incident X-ray energy is varied  
368 across an absorption edge (e.g.,  $K$  or  $L_I$ ,  $L_{II}$ ,  $L_{III}$ , etc.). A sharp change in the transmitted (and  
369 fluoresced) signal occurs when the energy of the incident photon corresponds to the energy  
370 of a shell of the absorbing atom. The spectral region containing this "white line", which is the  
371 intense feature within about 10 eV of this absorption threshold position, and the features  
372 within ~50 eV above this threshold, is referred to as the X-ray absorption near edge structure  
373 (XANES). XANES data are typically used to obtain information regarding the oxidation state  
374 and site symmetry of the absorbing atom. The spectral region extending from ~50 eV to  
375 ~1000 eV above the absorption threshold is referred to as the X-ray absorption fine structure  
376 (XAFS). XAFS is typically used to obtain structural information such as separations (e.g.,  
377 bond lengths) and coordination numbers of atom pairs in the structure for the absorbing  
378 element. In the case of amorphous materials, the information from XAFS is typically limited

379 to length scales that are part of the SRO. Further, when used with amorphous or disordered  
380 materials, XAFS has the problem of inaccuracy in terms of atom-pair distances and  
381 coordination numbers (see Crozier et al., 1988). Nevertheless, XAS methods can provide an  
382 ideal complement to bulk structural data based on scattering measurements because they are  
383 element-specific and are suitable even when the element of interest is at low concentration  
384 (usually down to 10's of ppm) in a sample.

385 A comprehensive review of XAS methods and applications in mineralogy and  
386 geochemistry can be found in Brown et al. (1988) and Henderson et al., (2014).

387 Finally, recent development of a TEM-based technique known as fluctuation electron  
388 microscopy (FEM), which is a hybrid imaging-diffraction method (Treacy et al., 2005), is  
389 proving to also be a valuable tool in studying the structures of amorphous materials. FEM  
390 can provide specific sensitivity to MRO of an amorphous material and has the advantage of  
391 sampling from small sample volumes. Recent FEM studies of amorphous silicon (a-Si)  
392 indicate the presence of paracrystalline ordered regions (that is showing SRO and MRO, but  
393 not LRO) in the 1 to 2 nm length scale (Treacy and Borisenko, 2012a), a provocative finding  
394 (Roorda and Lewis, 2012; Treacy and Borisenko, 2012b) that challenges the widely accepted  
395 notion that the structure of a-Si is well represented by the continuous random network (CRN)  
396 model. To date, FEM has been applied mainly to materials of technological interest such as  
397 amorphous semiconductors, disordered carbons, and metallic glasses (see Borisenko et al.  
398 2012, and references therein). We anticipate that future FEM studies will begin to include  
399 structural characterization of amorphous and poorly crystallized components in natural solids  
400 collected from environmental systems.

401 Experimental data derived from these various methods are analyzed via  
402 computational approaches that include molecular dynamics (MD), density functional theory  
403 (DFT), (reverse) Monte Carlo methods, and empirical potential structure refinement (EPSR),  
404 to name just a few.

#### 405 **Nanominerals, mineral nanoparticles and colloids**

406 Natural nanosized particles in environmental systems have been studied for decades  
407 and are an important part of the range of environmental colloids (Stumm and Morgan, 1970).  
408 In the full colloids category, a myriad of organic, inorganic, and organic/inorganic mixed  
409 particles with one or more dimensions in the 1 nm to 1 $\mu$ m size range are covered. However,  
410 especially in the last decade, a new field of study restricted to nanoscale minerals and mineral  
411 nanoparticles, known as nanomineralogy, is growing apart from the traditional colloidal

412 fields. The foundational characteristic of nanominerals (minerals only existing in the  
413 nanoscale) and mineral nanoparticles is to have at least one dimension spanning the range of  
414 1 nm to 100 nm; however, it is the often dramatic change in their physical and chemical  
415 properties as a function of their size that makes them unique in nature. Among the vast recent  
416 literature covering these phenomena, some representative examples are: up to two orders of  
417 magnitude faster  $Mn^{2+}$  oxidation rates per surface area due to smaller nanoparticulate iron  
418 oxide catalysis (comparing 7 nm vs. 37 nm hematite nanocrystals; Madden and Hochella,  
419 2005), higher phytotoxicity of ZnO nanoparticles compared with micrometer ZnO particles at  
420 equivalent concentrations (Yuwono et al., 2010), titanium dioxide mineral dissolution rates  
421 as a function of size (Schmidt and Vogelsberger, 2006),

422 It is worth noting that the recent remarkable increase in the study of nanominerals and  
423 mineral nanoparticles is attributed not only to their numerous applications in nanotechnology,  
424 but also to the fact that nanominerals and mineral nanoparticles are excellent natural proxies  
425 to assess the behavior and potential environmental risks of their anthropogenic counterparts.  
426 In this respect, many examples of the role played by mineral nanoparticles in the  
427 environment are continuously appearing (see compilations and perspectives by, e.g.,  
428 Hochella et al., 2008; Maurice and Hochella, 2008; Qafoku, 2010, 2011; Barnard and Guo,  
429 2012; and Barrón and Torrent, 2013) at the same time that individual nanominerals are being  
430 importantly scrutinized as never before, such as imogolite (Yuan and Wada, 2012),  
431 ferrihydrite (e.g. Michel et al., 2007; Manceau, 2011; Eusterhues et al., 2008; Gilbert et al.,  
432 2013), and schwertmannite (Fernandez-Martinez et al., 2010; French et al., 2012).  
433 Waychunas and others provide particularly useful and illustrative summaries of the chemistry  
434 and physics of the unique nature of mineral nanoparticles (Waychunas et al., 2005;  
435 Waychunas and Zhang, 2008).

436 Crystallinity and disorder play an essential role in influencing the specific behavior of  
437 nanominerals and mineral nanoparticles. It is well known that as the size of a nanoparticle is  
438 decreased, a much higher percentage of the mineral structure is at or near the surface.  
439 Notwithstanding, the study of the position of atoms, vacancies and defects at the surface of  
440 nanoparticles and nanominerals remains elusive and mostly unexplored. Some of the most  
441 advanced work at the forefront of this topic shows how mineral nanoparticles and  
442 nanominerals typically exhibit structural relaxation (inducing internal disorder and strain)  
443 that can vary with decreasing particle size and changes in composition (e.g., Drits and  
444 Tchoubar, 1990; Lanson et al., 2002; Gilbert et al., 2004; Drits et al., 2005; Michel et al.,

445 2007; Michel et al., 2010; Gilbert et al., 2013; Manceau et al., 2013). Along this same line of  
446 reasoning, it has been proposed that mineral nanoparticles can undergo internal structural  
447 changes as a response to changes in the surface environment (Zhang et al., 2003). In addition,  
448 the presence of nanoscale pores (also know as “nanopipes”, only 1-3 nanometers in diameter)  
449 have recently been observed in 10 to 40 nm hematite nanoparticles by means of HRTEM and  
450 3D electron tomography based on HAADF-STEM imaging (Echigo et al., 2013). The  
451 existence of these “nanopipes” enhances mineral dissolution by extending within the  
452 nanoparticle the commonly highly reactive sites at its surface.

453 The studies mentioned above also suggest that atomic structure, and particularly the  
454 role of surface and near-surface atomic structure modifications, must play a role in the  
455 kinetics of reactions of interest; but importantly also in the overall thermodynamic stability  
456 fields for the phases of key interest. This idea has been around for many decades, most  
457 notably demonstrated (in principal, and in a geochemical context) in a pioneering article by  
458 Langmuir (1971). But it has not been until relatively recently that the system  
459 thermodynamics primarily for anhydrous and hydrated transition metal oxides has been  
460 quantitatively and reliably worked out (Navrotsky et al., 2008, 2010; Navrotsky, 2011). The  
461 primary importance of this work is the realization that surface enthalpy becomes a critical  
462 factor in the thermodynamic stability of polymorphs or within a family of related minerals  
463 (e.g. iron oxides) as one moves from the micron to the nanometer size regime. The upshot is  
464 that phases only metastable in larger sizes may become thermodynamically  
465 stabilized/prefered at the nanoscale. Caution is in order here, in that in real environmental  
466 systems intrinsic factors (varying defect states, chemical impurities, phase heterogeneity,  
467 etc.) and extrinsic factors (e.g. system pH, Eh, and various organic and inorganic sorbents  
468 besides, or in addition to water) will potentially all adjust thermodynamic phase stability  
469 boundaries. Yet, it is the principle and landscape of both kinetic and thermodynamic affects  
470 that are important to realize here, if not to exactly understand or measure, but to at least  
471 appreciate their influence on the overall environmental system.

#### 472 **Amorphous-nanocrystalline transitional phases**

473 Definitions, categories, classifications, and structural models are convenient (and  
474 useful) human constructs, but not necessarily what nature presents to us. Nevertheless, Figure  
475 2 attempts to incorporate the latest thinking in the progression of materials between SRO,  
476 MRO, and LRO states. We admit that even this more complex view presented in Figure 2 is  
477 an oversimplification, but hopefully it is closer to what nature presents to us compared to

478 previous attempts at this sort of description. The most important point here, however, is that  
479 this view necessitates critical transitional states, or phases, which in any given system may be  
480 as influential, or more influential, than phases that are considered stable and often most  
481 abundant.

482 An example of these transitional phases is the recent redefinition of schwertmannite, a  
483 well-known natural material classified as a mineral, and recently more specifically as a  
484 “polyphasic nanomineral” (French et al., 2012). This new term was coined to describe the  
485 existence of two different nano-domains within schwertmannite nanoparticles (Fig. 1A).  
486 Using HRTEM, it was possible to differentiate goethite-like nano-domains within a  
487 preponderant amorphous sulfate-rich matrix, the combination giving us what it is known as  
488 schwertmannite. As suggested by French et al., the physical and chemical bulk response of a  
489 polyphasic nanomineral should reflect the characteristics and predominance of the different  
490 nano-domains. By the same token, for example, the solubility of polyphasic nanominerals  
491 has to be highly affected. Concerning this issue, an alternative thermodynamic model has  
492 been recently proposed combining the polyphasic nature of schwertmannite and a  
493 progressive solubility product range to reproduce the broad solubility of this nanomineral in  
494 nature (Caraballo et al., 2013).

495 Another important open aspect of this type of material is to elucidate a mechanism for  
496 polyphasic nanominerals formation. Although this specific case remains unclear, some other  
497 similar cases suggest non-classical nucleation in water-based solutions (Gebauer and Cölfen,  
498 2011) which need to be carefully considered. This is presented as an alternative option to the  
499 classical view of the crystallization process (different stages of crystallization proceeding via  
500 attachment of basic monomers like atoms, ions or molecules). This non-classical  
501 crystallization relies on polymers and the smallest nanoparticles as the primary crystal  
502 growth units. This construct effectively goes beyond, or must be considered in addition to,  
503 growth by oriented attachment of nanoparticles (Li et al, 2012, and references therein).  
504 Gebauer et al. (2008) first suggested that stable prenucleation calcium carbonate clusters are  
505 in fact the relevant species leading to the formation of different amorphous calcium  
506 carbonate phases that eventually will evolve into other crystalline calcium carbonates like  
507 calcite, vaterite, and aragonite. To date, no direct structural characterization of prenucleation  
508 clusters has been obtained, although recent studies are compiling indirect evidence for this  
509 phenomenon (Gebauer and Cölfen, 2011). Along these lines, cryogenic HRTEM and electron  
510 tomography have proven helpful in obtaining *in situ* images and 3D representations of



511 prenucleation clusters, as recently shown for calcium carbonates in aqueous solutions  
512 (Pouget et al., 2009) and calcium phosphate in simulated body fluids (Dey et al., 2010).  
513 However, paralleling this view is an alternative model known as liquid-liquid separation  
514 (reviewed and extended recently by Wallace et al., 2013). Supported by previous NMR, light  
515 scattering, and electron microscopy evidence, as well as spinodal decomposition theory and  
516 modeling, molecular dynamics simulations, and total x-ray pair distribution functions,  
517 Wallace et al. (2013) suggest that amorphous calcium carbonate (ACC) forms as a result of  
518 the formation of a dense liquid phase at a certain aqueous calcium carbonate ion activity  
519 product (depending on extrinsic conditions like temperature and pressure) via long-ago  
520 established spinodal decomposition principles. Coalescence and at least partial dehydration  
521 of these nanoscale clusters is suggested to result in the formation of the ACC phase.

522 Most recently, Lupulescu and Rimer (2014) used time-resolved atomic force  
523 microscope images under hydrothermal conditions to show that silicalite-1 (a siliceous ZSM-  
524 5 zeolite) grows in classical and non-classical pathways at the same time, by simultaneous  
525 accretion of silica molecules as the primary growth unit, but also by the aggregation of  
526 metastable silica nanoparticle precursors.

527 We suggest that all of these studies have vitally important developmental impact in  
528 aquatic systems where the presence of polymeric species and small clusters have previously  
529 been suggested, suspected, or confirmed. These include the prenucleation units of silicic acid  
530 polymers during the silicification process (Perry, 2003), as well as Al-Keggin polyoxocations  
531 in the origin of aluminum flocs in rivers bearing metal contaminants (Furrer et al., 2002). The  
532 incorporation of synchrotron X-ray scattering, the latest TEM methods, and a myriad of other  
533 analytic and experimental methods focused on the study of nucleation and growth of well  
534 known phases (as well as lesser known phases like polyphasic nanominerals) are expected to  
535 significantly advance the understanding of these important environmentally-relevant  
536 chemical phenomena.

### 537 **Mesocrystals**

538 Advances in crystallization pathways as discussed above, and also the developing  
539 science of nanophase oriented aggregation (Penn and Banfield, 1998; Banfield et al., 2000;  
540 Li et al., 2012), help in part to explain and visualize the formation of mesoscopically  
541 structured crystals, also referred to as mesocrystals. The highly oriented subunits forming a  
542 mesocrystal differentiate this material from polycrystals characterized by randomly oriented

543 units, whereas in both cases the identifiable nano-sized units distinguish them from single  
544 crystals. Several mechanisms of formation can generate mesocrystals, but at the same time  
545 they can lead to the formation of single crystals; therefore it is important to emphasize that  
546 the term mesocrystal defines the structure of a material rather than its exact formation  
547 mechanism. The number of mesocrystal-related studies has increased dramatically over the  
548 last decade with various comprehensive review articles periodically updating several stages  
549 of advances (Cölfen and Mann, 2003; Cölfen and Antonietti, 2005; Song and Cölfen, 2010).  
550 Four main mechanisms generating mesocrystals have been proposed to date (Fig. 2): a)  
551 alignment of nanoparticles by an oriented organic matrix, b) ordering by physical fields and  
552 interparticles forces, c) mineral bridges and d) space constraints. For a detailed discussion of  
553 the different mechanisms and specific cases, the reader is referred to Song and Cölfen (2010).

554         The specific case of oriented aggregation will be discussed here to illustrate once  
555 again the impressive advances in the understanding of mineral crystallinity as a result of  
556 technological progress. Oriented aggregation is a non-classical crystal growth mechanism  
557 that involves the self-assembly of primary nanocrystals, including crystallographic  
558 reorganization within the self-assemblies and conversion to oriented aggregates (Yuwono et  
559 al., 2010). The use of HRTEM has allowed for the direct observation of this non-classical  
560 crystallization mechanism for natural iron oxyhydroxides biomineralization products  
561 (Banfield et al., 2000). The next step in the understanding of this process was made possible  
562 by the application of cryogenic HRTEM (Yuwono et al., 2010). This technique enables direct  
563 observation of nanoparticles in aqueous suspension thanks to the preservation of the three-  
564 dimensional arrangement of nanoparticles as a result of water vitrification. However, more  
565 recently the actual observation of the aggregation, attachment and growth of ferrihydrite  
566 nanoparticles was finally achieved directly in aqueous solution and in real-time using  
567 HRTEM and a water-filled TEM environmental cell (Li et al., 2012). It was observed how, at  
568 the time of attachment, ferrihydrite nanoparticles shared the same crystallographic  
569 orientation with their neighbors (either exact structural alignment or twin-related), and how  
570 after the attachment event, atoms filled the interface region on a time scale on the order of 10  
571 to 100 s. This study also observed attachment and recrystallization of misaligned particles  
572 and dissolution of small particles in the vicinity of larger ones; showing that, even in systems  
573 where oriented attachment is dominant, classical crystallization process like Ostwald  
574 ripening can play an important role.

575 Another example of how the synergetic use of several techniques (HRTEM, NMR,  
576 FTIR and synchrotron XRD) is leading to a unique level of detail in the understanding of  
577 mineral crystallinity is shown in a recent study of the structure-property relationships of  
578 biological mesocrystals in the adult sea urchin spine (Seto et al., 2012). This study has shown  
579 how each spine comprises a highly oriented array of Mg-calcite nanocrystals in which  
580 amorphous regions and organic macromolecules are embedded. This case illustrates how  
581 complex hierarchical structures can diffract as a single crystal and yet fracture as a glassy  
582 material.

### 583 **IMPLICATIONS**

584 Our experience in looking at the environmental impacts of mining (Hochella et al.,  
585 1999, 2005a, 2005b, 2008; Plathe et al., 2010, 2013; French et al., 2012; Mantha et al., 2012;  
586 Schindler et al., 2012) have shown us repeatedly that whenever we look at the inorganic  
587 portion of environmental samples in detail with TEM, we invariably find 1) minerals that are  
588 known but that have not previously been reported in that environment; 2) minerals that show  
589 a wide range of crystallinity, some of which have never been described before; and 3)  
590 amorphous materials that have not been described before, and with compositions that range  
591 from simple to complex. Because these phases are minute, and/or often not highly crystalline,  
592 and/or less abundant, they are typically ignored or more likely missed altogether. Yet they  
593 can be (and most often are) highly relevant to important aspects of how the  
594 (bio)geochemistry of that system works, or how the system evolves with time, or how that  
595 system impacts the ecosystem in which it exists, as well as how they impact surrounding  
596 ecosystems. For example, in metal-contaminated mine-drainage systems that can extend tens  
597 to hundreds of kilometers, nanominerals and mineral nanoparticles can be highly reactive  
598 toxic metal sorbents, and in the case of very small nanoparticles, they can be hyper-reactive  
599 (O'Reilly and Hochella, 2003; Madden and Hochella, 2005; Hochella et al., 2005a; French et  
600 al., 2012; Caraballo et al., 2013). It has been shown that a hyper-reactive nanophase at just  
601 1% concentration can completely dominate a critical geochemical reaction in such a system  
602 (Fig. 1.2 in Hochella et al., 2012).

603 Independently, other groups have been able to also overcome many of the distinct  
604 challenges of sorting out the identification and assessment of key naturally-occurring  
605 nanomaterials in highly complex environmentally-relevant water systems. They have done so  
606 in a variety of ways, including: imaging and analytic techniques centered around synchrotron

607 x-ray methods and TEM's (as described in this paper), sophisticated filtering methods  
608 (tangential and flow field fractional methods), column experiments with natural samples,  
609 molecular biology assessments, sequential extraction, electrophoretic mobility methods, ICP-  
610 MS, NMR, Mossbauer spectroscopy, and so on. Key publications include Bertsch and  
611 Seaman (1999), Lead and Wilkinson (2006), Moreau et al. (2007), Theng and Yuan (2008),  
612 and Weber et al. (2009). The overarching theme of these papers, and some of the papers that  
613 they cite, is similar to ours, showing great and often unexpected mineral/biological  
614 complexity within natural soil, sediment, aquifer, and surface water systems at the nanometer  
615 to micron scale. Controlling influences of key (bio)geochemical reactions of interest (e.g.  
616 contaminant association and transport) often have not been predicted or even identified by  
617 idealized laboratory-based experiments or observations using a single or a few system  
618 components under idealized conditions. Even the most common or obvious minerals or  
619 organic/biological agents observed in the field are often not a controlling influence in the  
620 most interesting/important overall chemistry that is attempting to be understood. Further still,  
621 sub-nanometer science has even taken some interesting and unexpected turns. Fourier  
622 transform mass spectrometry and voltammetric analysis has been used to find, characterize,  
623 and sort out the importance of multinuclear clusters (e.g.  $M_3S_3$  or  $M_4S_6$ ), which are sub-  
624 nanometer in size (e.g. Rozan et al., 2000; Luther and Rickard, 2005). These clusters are  
625 what might be considered the very smallest of the nanoparticles with their own remarkable  
626 behaviors and environmental significance.

627       As all of the above studies have shown, non-crystalline and poorly crystalline  
628 materials, as well as nanomaterials in all degrees of crystallization, are typically much more  
629 difficult to find and to study in environmental samples that are invariably complex and very  
630 difficult with which to deal. Overall, this has resulted in a distinct under-representation of the  
631 studies that look at natural systems relative to the overall scientific production output within  
632 this field.

633       The technological revolution described herein is enabling the direct study of minerals  
634 and their formation in their natural environmental compartments, generating a more realistic  
635 understanding of their response to changes in the physical chemistry of the environmental  
636 system and vice versa. The next several years are also expected to experience a notable  
637 proliferation in the number of synchrotron, FEL and HRTEM "real time" studies intended to  
638 reveal non-classical crystallization pathways. These studies, among other things, should be

639 able to unravel the role of polymers and prenucleation clusters in the early stages of mineral  
640 formation.

641 Mineral thermodynamics, reaction kinetics, and solubility are other research areas  
642 where a deep influence of future discoveries in mineral crystallinity can be anticipated. To  
643 this end, it is compelling to obtain a better understanding of nanomineral and mineral  
644 nanoparticle singular characteristics, such as crystal structure, surface disorder, nano-  
645 domains, nano-porous heterogeneity, and 3D morphologies.

646 The varied, unique, and/or sometimes highly complex characteristics of mesocrystals  
647 (e.g., high crystallinity and porosity, nanocrystalline individual subunits or organic-inorganic  
648 hybrid structures) enhance their functionality (including in living systems) compared to their  
649 single crystal counterparts. The discovery of new naturally occurring mesocrystals, as well as  
650 a deeper understanding of their formation mechanisms, will allow us to transfer their special  
651 properties to new synthetic and biomimetic materials.

652 The forthcoming discoveries in mineral crystallinity within complex environmental  
653 systems will have a significant effect on the understanding of the roles played in nature by  
654 amorphous and nano-sized neoformed mineral phases, mineral nanoparticles, and  
655 mesocrystals. In addition, this will have an important impact in other areas like material  
656 sciences and nanotechnology where natural materials and processes will likely inspire new  
657 synthetic materials and nanotechnological applications.

658

659

## ACKNOWLEDGMENTS

660 M.A.C. was financially supported by the Spanish Ministry of Education and the Post-  
661 doctoral International Mobility Sub-programme I+D+i 2008-2011. Grants from the U.S.  
662 Department of Energy (DE-FG02-06ER15786) and the Institute for Critical Technology and  
663 Applied Sciences at Virginia Tech also provided financial support for this project. We are  
664 also appreciative of the support from the National Science Foundation (NSF) and the  
665 Environmental Protection Agency through the Center for Environmental Implications of  
666 NanoTechnology (CEINT) funded under NSF Cooperative Agreement EF-0830093. We  
667 would also like to thank four anonymous reviewers and especially Dr. Alejandro Fernández-  
668 Martínez (Associate Editor) for their many and thoughtful comments that significantly  
669 improved the quality of this paper.

670

671

## REFERENCES

- 672 Banfield, J.F., Welch, S.A., Zhang, H., Ebert, T.T., and Penn, R.L. (2000) Aggregation-based  
673 crystal growth and microstructure development in natural iron oxyhydroxide  
674 biomineralization products. *Science*, 289, 751-754.
- 675 Barnard, A.S., and Guo, H. (2012) *Nature's Nanostructures*. Pan Stanford Publishing Pte.  
676 Ltd., USA.
- 677 Barton, B., Jiang, B., Song, C., Specht, P., Calderon, H., and Kisielowski, C. (2012) Atomic  
678 Resolution Phase Contrast Imaging and In-Line Holography Using Variable Voltage  
679 and Dose Rate. *Microscopy and Microanalysis*, 18, 982-994.
- 680 Barrón, V. and Torrent, J. (2013) Iron, manganese and aluminum oxides and oxyhydroxides.  
681 *European Mineralical Union Notes in Mineralogy*, v. 14, Chapter 9, 297-336.
- 682 Bertsch, P.M., and J.C. Seaman (1999) Characterization of complex mineral assemblages:  
683 Implications for contaminant transport and environmental remediation. *Proceedings*  
684 *of the Natural Academy of Science*, 96, 3350-3357.
- 685 Billinge, S.J.L. (2004) The atomic pair distribution function: Past and present. *Zeitschrift für*  
686 *Kristallographie*, 219, 117-121.
- 687 Bindi, L. and Steinhardt, P.J. (2012) The discovery of the first natural quasicrystal.  
688 *Elements*, 8, 13-14.
- 689 Bindi, L., Steinhardt, P.J., Yao, N., and Lu, P.J. (2011) Icosahedrite,  $Al_{63}Cu_{24}Fe_{13}$ , the first  
690 natural quasicrystal. *American Mineralogist*, 96, 928-931.
- 691 Borisenko, K.B., Haberl, B., Liu, A.C.Y., Chen, Y., Li, G., Williams, J.S., Bradby, J.E.,  
692 Cockayne, D.J.H., Treacey, M.M.J. (2012) Medium-range order in amorphous silicon  
693 investigated by constrained structural relaxation of two-body and four-body electron  
694 diffraction data. *Acta Materialia*, 60, 359-375.
- 695 Bragg, W.L. (1912) The Specular Reflexion of X-rays. *Nature* 90 (2250): 410
- 696 Brown, G.E., Jr., Calas, G., and Waychunas, G.A. (1988) X-ray absorption spectroscopy and  
697 its applications in mineralogy and geochemistry. In F.C. Hawthorne, Ed., *Reviews in*  
698 *Mineralogy and Geochemistry, Spectroscopic Methods in Mineralogy and Geology*,  
699 18, p. 431-512. Mineralogical Society of America, Geochemical Society, Chantilly,  
700 Virginia.

- 701 Caraballo, M.A., Rimstidt, J.D., Macías, F., Nieto, J.M., and Hochella, M.F. Jr. (2013)  
702 Metastability, nanocrystallinity and pseudo-solid solution constraints to  
703 schwertmannite solubility. *Chemical Geology*, 360/361, 22-31.
- 704 Cölfen, H., and Antonietti, M. (2005) Mesocrystals: Inorganic superstructures made by  
705 highly parallel crystallization and controlled alignment. *Angewandte Chemie*  
706 *International Edition*, 44, 5576-5591.
- 707 Cölfen, H., and Mann, S. (2003) Higher-order organization by mesoscale self-assembly and  
708 transformation of hybrid nanostructures. *Angewandte Chemie International Edition*,  
709 42, 2350-2365.
- 710 Crozier, D.E., Rehr, J. J. & Ingalls, R. (1988). *X-ray Absorption: Principles, Applications,*  
711 *Techniques of EXAFS, SEXAFS and XANES*, edited by D. C. Kononsberger & R.  
712 Prins, ch. 9. New York: Wiley.
- 713 Debye, P. (1915) Dispersion of röntgen rays. *Annalen der Physik*, 46, 809.
- 714 Dey, A., Bomans, P.H.H., Müller, F.A., Will, J., Frederik, P.M., de With, G., and  
715 Sommerdijk, N.A.J.M. (2010) The role of prenucleation clusters in surface-induced  
716 calcium phosphate crystallization. *Nature Materials*, 9, 1010-1014.
- 717 Dove, M.T. (2002) An introduction to the use of neutron scattering methods in mineral  
718 sciences. *European Journal of Mineralogy*, 14, 203-224.
- 719 Drits, V.A., Sakharov, B.A., Salyn, A.L., and Lindgreen, H. (2005) Determination of the  
720 content and distribution of fixed ammonium in illite-smectite using a modified X-ray  
721 diffraction technique: Application to oil source rocks of western Greenland.  
722 *American Mineralogist*, 90, 71-84.
- 723 Drits, V.A. and Tchoubar, C. (1990) X-ray diffraction by disordered lamellar structures:  
724 Theory and applications to microdivided silicates and carbons. 371 p. Springer-  
725 Verlag, Berlin.
- 726 Echigo, T., Monsegue, N., Aruguete, D.M., Murayama, M., and Hochella, M.F. (2013)  
727 Nanopores in hematite ( $\alpha$ -Fe<sub>2</sub>O<sub>3</sub>) nanocrystals observed by electron tomography.  
728 *American Mineralogist*, 98, 154-162.
- 729 Egami, T. and Billinge, S.J.L. (2003) *Underneath the Bragg Peaks: Structural Analysis of*  
730 *Complex Materials*. Oxford, Pergamon Press.

- 731 Eusterhues, K., Wagner, F. E., Hausler, W., Hanzlik, M., Knicker, H., Totsche, K. U., Kogel-  
732 Knabner, I., and Schwertmann, U. (2008). Characterization of ferrihydrite-soil  
733 organic matter coprecipitates by X-ray diffraction and Mossbauer spectroscopy.  
734 Environmental Science and Technology 42, 7891–7897.
- 735 Fernandez-Martinez, A., Timon, V., Roman-Ross, G., Cuello, G.J., Daniels, J.E., Ayora, C.  
736 (2010) The structure of schwertmannite, a nanocrystalline iron oxyhydroxysulfate.  
737 American Mineralogist, 95, 1312-1322.
- 738 French, R.A., Caraballo, M.A., Kim, B., Rimstidt, J.D., Murayama, M., and Hochella, M.F.,  
739 Jr. (2012) The enigmatic iron oxyhydroxysulfate nanomineral schwertmannite:  
740 Morphology, structure, and composition. American Mineralogist, 97, 1469-1482.
- 741 Furrer, G., Phillips, B.L., Ulrich, K.U., Pöthig, R., and Casey, W.H. (2002) The origin of  
742 aluminum flocs in polluted streams. Science, 297, 2245-2247.
- 743 Gebauer, D., and Cölfen, H. (2011) Prenucleation clusters and non-classical nucleation. Nano  
744 Today, 6, 564-584.
- 745 Gebauer, D., Völkel, A., and Cölfen, H. (2008) Stable prenucleation calcium carbonate  
746 clusters. Science, 322, 1819-1822.
- 747 Gilbert, B., Huang, F., Zhang, H., Waychunas, G.A., and Banfield, J.F. (2004) Nanoparticles:  
748 Strained and stiff. Science, 305, 651-654.
- 749 Gilbert, B., Erbs, J.J., Penn, R.L., Petkov, V., Spagnoli, D., Waychunas, G.A. (2013) A  
750 disordered nanoparticle model for 6-line ferrihydrite. American Mineralogist, 98,  
751 1465-1476.
- 752 Goodwin, A.L., Michel, F.M., Phillips, B.L., Keen, D.A., Dove, M.T., and Reeder, R.J.  
753 (2010) Nanoporous structure and medium-range order in synthetic amorphous  
754 calcium carbonate. Chemistry of Materials, 22, 3197-3205.
- 755 Henderson, G.S., Neuvill, D.R., and Downs, R. (2014) Spectroscopic methods in  
756 mineralogy and material sciences, 78, p. 1-801. In J.J. Rosso, Ed. Mineralogical  
757 Society of America, Geochemical Society, Chantilly, Virginia.
- 758 Hochella, M.F., Jr., Moore, J.N., Golla, U., and Putnis, A. (1999) A TEM study of samples  
759 from acid mine drainage systems: Metal - mineral association with implications for  
760 transport. Geochimica et Cosmochimica Acta, 63, 3395-3406.



- 761 Hochella M.F., Jr., Kasama T., Putnis A., Putnis C., and Moore J.N. (2005a)  
762 Environmentally important, poorly crystalline Fe/Mn hydrous oxides: Ferrihydrite  
763 and a possibly new vernadite-like mineral from the Clark Fork River Superfund  
764 Complex. *American Mineralogist*, 90, 718-724.
- 765 Hochella, M.F., Jr., Moore J.N., Putnis C., Putnis A., Kasama T., and Eberl D.D. (2005b)  
766 Direct observation of heavy metal-mineral association from the Clark Fork River  
767 Superfund Complex: Implications for metal transport and bioavailability.  
768 *Geochimica et Cosmochimica Acta*, 69, 1651-1663.
- 769 Hochella, M.F., Jr., Lower, S.K., Maurice, P.A., Penn, R.L., Sahai, N., Sparks, D.L., and  
770 Twining, B.S. (2008) Nanominerals, mineral nanoparticles, and Earth systems.  
771 *Science*, 319, 1631-1635.
- 772 Hochella, M.F. Jr., Aruguete, D., Kim, B., and Madden A.S. (2012) Naturally occurring  
773 inorganic nanoparticles: General assessment and a global budget for one of Earth's  
774 last unexplored geochemical components. In: *Nature's Nanostructures*, pp. 1-42 (A.S.  
775 Barnard, H. Guo, Eds.) Pan Stanford Publishing, Singapore.
- 776 International Union of Crystallography, Report of the Executive Committee for 1991), *Acta*  
777 *Crystallographica A*48 (1992) 922-946.
- 778 Klein, C. and Dutrow, B. (2008) *Mineral Science*. Wiley, New York.
- 779 Klug, H.P. and Alexander, L.E. (1974) *X-ray Diffraction Procedures for Poly-crystalline\_ and*  
780 *Amorphous Materials*. Wiley, New York, 2<sup>nd</sup> edition.
- 781 Langmuir, D. (1971) Particle size effect on the reaction goethite = hematite + water.  
782 *American Journal of Science*, 271, 147-156.
- 783 Lanson, B., Drits, V.A., Gaillot, A.C., Silvester, E., Plançon, A., and Manceau, A. (2002)  
784 Structure of heavy-metal sorbed birnessite: Part 1. Results from X-ray diffraction.  
785 *American Mineralogist* 87, 1631-1645.
- 786 Lead, J.R. and K.J. Wilkinson (2006) Aquatic colloids and nanoparticles: Current knowledge  
787 and future trends. *Environmental Chemistry*, 3, 159-171.

- 788 Li, D., Nielsen, M.H., Lee, J.R.I., Frandsen, C., Banfield, J.F., and De Yoreo, J.J. (2012)  
789 Direction-specific interactions control crystal growth by oriented attachment. *Science*,  
790 336, 1014-1018.
- 791 Lin, J.F., Sturhahn, W., Zhao, J., Shen, G., Mao, H.K. and Hemley, R.J. (2005) Sound  
792 velocities of hot dense iron: Birch's Law revisited. *Science* 308: 1892-1894.
- 793 Loh, N.D., Hampton, C.Y., Martin, A.V., Starodub, D., Sierra, R.G., Barty, A., Aquila, A.,  
794 Schulz, J., Lomb, L., Steinbrener, J., Shoeman, R.L., Kassemeyer, S., Bostedt, C.,  
795 Bozek, J., Epp, S.W., Erk, B., Hartmann, R., Rolles, D., Rudenko, A., Rudek, B.,  
796 Foucar, L., Kimmel, N., Weidenspointner, G., Hauser, G., Holl, P., Pedersoli, E.,  
797 Liang, M., Hunter, M.M., Gumprecht, L., Coppola, N., Wunderer, C., Graafsma, H.,  
798 Maia, F.R.N.C., Ekeberg, T., Hantke, M., Fleckenstein, H., Hirsemann, H., Nass, K.,  
799 White, T.A., Tobias, H.J., Farquar, G.R., Benner, W.H., Hau-Riege, S.P., Reich, C.,  
800 Hartmann, A., Soltau, H., Marchesini, S., Bajt, S., Barthelmess, M., Bucksbaum, P.,  
801 Hodgson, K.O., Struder, L., Ullrich, J., Frank, M., Schlichting, I., Chapman, H.N.,  
802 and Bogan, M.J. (2012) Fractal morphology, imaging and mass spectrometry of  
803 single aerosol particles in flight. *Nature*, 486, 513-517.
- 804 Lucovsky, G. (1987) Specification of medium range order in amorphous materials. *Journal of*  
805 *Non-Crystalline Solids*, 97-98, 155-158.
- 806 Luther, G.W. III and Rickard, D.T. (2005) Metal sulfide cluster complexes and their  
807 biogeochemical importance in the environment. *Journal of Nanoparticle Research*, 7,  
808 389-407.
- 809 Lupulescu, A.I. and Rimer, J.D. (2014) In situ imaging of silicalite-1 surface growth reveals  
810 the mechanism of crystallization. *Science*, 344, 729-732.
- 811 Lytle, F.W. (1999) The EXAFS family tree: A personal history of the development of X-ray  
812 absorption fine structure. *Journal of Synchrotron Radiation*, 6, 123-134.
- 813 Madden, A.S., and Hochella Jr, M.F. (2005) A test of geochemical reactivity as a function of  
814 mineral size: Manganese oxidation promoted by hematite nanoparticles. *Geochimica*  
815 *et Cosmochimica Acta*, 69, 389-398.
- 816 Majzlan, J., and Myneni, S.C.B. (2005) Speciation of iron and sulfate in acid waters:  
817 Aqueous clusters to mineral precipitates. *Environmental Science and Technology*,  
818 39(1), 188-194.

- 819 Manceau, A. (2011) Critical evaluation of the revised akdalaite model for ferrihydrite.  
820 American Mineralogist, 96, 521-533.
- 821 Manceau, A., Marcus, M.S., Grangeon, S., Lanson, M., Lanson, B., Gaillot, A.C.,  
822 Skanthakumar, S., Solderholme, L. (2013) Short-range and long-range order of  
823 phyllomanganate nanoparticles determined by high-energy X-ray scattering. Journal  
824 of Applied Crystallography, 46, 193-209.
- 825 Mantha N., Schindler M., Murayama M., and Hochella M.F., Jr. (2012) Silica- and sulfate-  
826 bearing rock coatings in smelter areas: Products of chemical weathering and  
827 atmospheric pollution. I. Formation and mineralogical composition. Geochimica et  
828 Cosmochimica Acta, 85, 254-274.
- 829 Maurice P.A. and Hochella M.F. Jr. (2008) Nanoscale Particles and Processes: A New  
830 Dimension in Soil Science. Advances in Agronomy 100, 123-153. D.L. Sparks,  
831 Editor. Elsevier, Inc.
- 832 Michel, F.M., Ehm, L., Sytle, M.A., Lee, P.L., Chupas, P.J., Liu, G., Strongin, D.R.,  
833 Schoonen, M.A.A., Phillips, B.L., and Parise, J.B. (2007) The structure of  
834 ferrihydrite, a nanocrystalline material. Science, 316, 1726.
- 835 Michel, F. M., MacDonald, J. Feng, J., Phillips, B. L., Ehm, L., Tarabrella, C., Parise, J. B., &  
836 Reeder, R. J. (2008) Structural characteristics of synthetic amorphous calcium  
837 carbonate. Chemistry of Materials, 20, 4720-4728.
- 838 Michel, F. M., Barrón, V., Torrent, J., Morales, M. P., Serna, C. J., Boily, J. -F., Liu, Q.,  
839 Ambrosini, A., Cismasu, C. A., Brown, Jr., G. E. (2010) Ordered ferrimagnetic form  
840 of ferrihydrite reveals links among structure, composition, and magnetism,  
841 Proceedings of the National Academy of Sciences of The United States of America,  
842 107, 2787-2792.
- 843 Monsegue, N., Reynolds, W.T. Jr., Hawk, J.A., and Murayama, M. (in press) How TEM  
844 projection artifacts distort microstructure measurements: A case study in a 9% Cr-  
845 Mo-V steel. Metallurgical and Materials Transactions A.
- 846 Moreau, J. W., Weber, P. K., Martin, M. C., Gilbert, B., Hutcheon, I. D., and Banfield, J. F.  
847 (2007) Extracellular proteins limit the dispersal of biogenic nanoparticles. Science,  
848 316, 1600-1603.

- 849 Navrotsky, A. (2011) Nanoscale effects on thermodynamics and phase equilibria in oxide  
850 systems. *ChemPhysChem*, 12, 2207-2215.
- 851 Navrotsky, A., Mazeina, L., and Majzlan, J. (2008) Size-driven structural and  
852 thermodynamic complexity in iron oxides. *Science*, 319, 1635-1638.
- 853 Navrotsky, A., Ma, C., Lilova, K., and Birkner, N. (2010) Nanophase transition metal oxides  
854 show large thermodynamically driven shifts in oxidation-reduction equilibria.  
855 *Science*, 330, 199-201.
- 856 Nickel, E.H. (1995). Definition of a mineral. *Canadian Mineralogist*, 33, 689-690.
- 857 O'Reilly, S.E. and Hochella, M.F., Jr. (2003) Lead sorption efficiencies of natural and  
858 synthetic Mn and Fe-oxides. *Geochimica et Cosmochimica Acta*, 67, 4471-4487.
- 859 Penn, R.L. and Banfield, J.F. (1998) Imperfect oriented attachment: Dislocation generation in  
860 defect-free nanocrystals. *Science*, 281, 969-971.
- 861 Perry, C.C. (2003) Silicification: The processes by which organisms capture and mineralize  
862 silica. In J.J. Rosso, Ed., *Reviews in Mineralogy and Geochemistry*,  
863 *Biom mineralization*, 54, p. 291-327. Mineralogical Society of America, Geochemical  
864 Society, Chantilly, Virginia.
- 865 Plathe, K.L., von der Kammer, F., Hassellöv, M., Moore, J., Mura Salmonyama, M.,  
866 Hofmann, T., and Hochella, M.F., Jr. (2010) Using FIFFF and aTEM to determine  
867 trace metal – nanoparticle associations in riverbed sediment. *Journal of*  
868 *Environmental Chemistry* 7, 82-93.
- 869 Plathe, K.L., von der Kammer, F., Hasselov, M., Moore, J.N. Murayama, M., Hofmann, T.,  
870 Hochella, M.F., Jr. (2013) The role of nanominerals and mineral nanoparticles in the  
871 transport of toxic trace metals: Field-flow fractionation and analytical TEM analyses  
872 after nanoparticle isolation and density separation. *Geochimica et Cosmochimica*  
873 *Acta*, 102, 213-225.
- 874 Pouget, E.M., Bomans, P.H.H., Goos, J.A.C.M., Frederik, P.M., de With, G., and  
875 Sommerdijk, N.A.J.M. (2009) The initial stages of template-controlled CaCO<sub>3</sub>  
876 formation revealed by Cryo-TEM. *Science*, 323, 1455-1458.
- 877 Poulsen, H.F., Neufeind, J., Neumann, H.-B., Schneider J.R., and Zeidler, M.D. (1995)  
878 Amorphous silica studied by high energy X-ray diffraction. *Journal of Non-*  
879 *Crystalline Solids*, 188, 63-74.

- 880 Proffen, T. (2006) Analysis of disordered materials using total scattering and the pair  
881 distribution function.  
882  
883 in *Mineralogy and Geochemistry*, 63, 255-274.
- 884 Qafoku, N.P. (2010) Terrestrial nanoparticles and their controls on soil-/geo-processes and  
885 reactions. In Donald L. Sparks, editor: *Advances in Agronomy*, Vol. 107, Burlington:  
886 Academic Press, pp. 33-91.
- 887 Qafoku, N.P. (2011) Impacts of environmental nanoparticles on physical, chemical,  
888 biological and hydrological processes in terrestrial ecosystems. In *Handbook of Soil  
889 Sciences: Resource Management and Environmental Impacts*, Second Edition (P.M.  
890 Huang, Y. Li, M.E. Sumner, Eds.), CRC Press, pp. 4-1 to 4-18.
- 891 Radha, A.V., Fernandez-Martinez, A., Hu, Y., Jun, Y.-S., Waychunas, G.A., and Navrotsky,  
892 A. (2012) Energetic and structural studies of amorphous  $\text{Ca}_{1-x}\text{Mg}_x\text{CO}_3 \cdot n\text{H}_2\text{O}$  ( $0 \leq x \leq$   
893  $1$ ). *Geochimica et Cosmochimica Acta*, 90, 83-95.
- 894 Reeder, R.J., Tang, Y., Schmidt, M.P., Kubista, L.M., Cowan, D.F., Phillips, B.L. (2013)  
895 Characterization of structure in biogenic amorphous calcium carbonate: Pair  
896 distribution function and nuclear magnetic resonance studies of lobster gastrolith.  
897 *Crystal Growth & Design*, 13, 1905-1914.
- 898 Rickerby, D.G., Valdrè, G., and Valdrè, U. (1999) Impact of electron and scanning probe  
899 microscopy on materials research. Kluwer Academic Publisher, Dordrecht,  
900 Netherlands.
- 901 Rietveld, H.M. (1969) A profile refinement method for nuclear and magnetic structures.  
902 *Journal of Applied Crystallography*, 2, 65-71.
- 903 Roorda, S. and Lewis, L.J. (2012) Comment on “The local structure of amorphous silicon”.  
904 *Science*, 338, 1539b.
- 905 Rozan, T.F., Lassman, M.E., Ridge, D.P., Luther, G.W. III (2000) Evidence for iron, copper  
906 and zinc complexation as multinuclear sulphide clusters in oxic rivers. *Nature*, 406,  
907 879-882.

- 908 Schindler M., Mantha N., Keyser K.T., Murayama M., and Hochella M.F., Jr. (2012) Shining  
909 light on black rock coatings in smelter impacted areas. *Geoscience Canada*, 39, 148-  
910 157.
- 911 Schmidt, J., and Vogelsberger, W. (2006) Dissolution kinetics of titanium dioxide  
912 nanoparticles: The observation of an unusual kinetic size effect. *The Journal of*  
913 *Physical Chemistry B*, 110, 3955-3963.
- 914 Scott, M. C., Chen, C.-C., Mecklenburg, M., Zhu, C., Xu, R., Ercius P., Dahmen, U., Regan,  
915 B. C., and Miao, J. (2012) Electron tomography at 2.4-angstrom resolution. *Nature*,  
916 483, 444-448.
- 917 Seto, J., Ma, Y., Davis, S.A., Meldrum, F., Gourrier, A., Kim, Y.-Y., Schilde, U., Sztucki,  
918 M., Burghammer, M., Maltsev, S., Jäger, C., and Cölfen, H. (2012) Structure-  
919 property relationships of a biological mesocrystal in the adult sea urchin spine.  
920 *Proceedings of the National Academy of Sciences*. Published ahead of print February  
921 16, 2012, doi:10.1073/pnas.1109243109.
- 922 Song, R.-Q., and Cölfen, H. (2010) Mesocrystals—Ordered nanoparticle superstructures.  
923 *Advanced Materials*, 22, 1301-1330.
- 924 Stumm, W., and Morgan, J.J. (1970) *Aquatic Chemistry: An introduction emphasizing*  
925 *chemical equilibria in natural waters*. Wiley-Interscience, New York.
- 926 Sutton, S.R. (2006) User research facilities in Earth Sciences. *Elements*, 2, 1-64.
- 927 Theng, B.K.G. and Yuan, G.D. (2008) Nanoparticles in the soil environment. *Elements* 4,  
928 395-399.
- 929 Trainor, T.P., Chaka, A.M., Eng, P.J., Newville, M., Waychunas, G.A., Catalano, J.G.,  
930 Brown, Jr., G.E. (2004) Structure and reactivity of the hydrated hematite (0001)  
931 surface. *Surface Science*, 573, 204-224.
- 932 Treacy, M.M.J, Gibson, J.M., Fan, L., Paterson, D.J., McNulty, I. (2005) Fluctuation  
933 microscopy: a probe of medium range order. *Reports on Progress in Physics*, 68,  
934 2899-2944.
- 935 Treacy, M.M.J. and Borisenko, K.B. (2012a) The local structure of amorphous silicon.  
936 *Science*, 335, 950-953.

- 937 Treacy, M.M.J. and Borisenko, K.B. (2012b) Response to Comment on “The local structure  
938 of amorphous silicon”. *Science*, 338, 1539c.
- 939 Ullrich, J., Rudenko, A., and Moshhammer, R. (2012) Free-electron lasers: New avenues in  
940 molecular physics and photochemistry. *Annual Review of Physical Chemistry*, 63,  
941 635-660.
- 942 Van Aert, S., Batenburg, K.J., Rossell, M.D., Erni, R., and Van Tendeloo, G. (2011) Three-  
943 dimensional atomic imaging of crystalline nanoparticles. *Nature*, 470, 374-377.
- 944 Van Dyck, D., and Chen, F.-R. (2012) ‘Big Bang’ tomography as a new route to atomic-  
945 resolution electron tomography. *Nature*, 486, 243-246.
- 946 Wallace, A.F., Hedges, L.O., Fernandez-Martinez, A., Raiteri, P., Gale, J.D., Waychunas,  
947 G.A., Whitlam, S., Banfield, J.F., De Yoreo, J.J. (2013) Microscopic evidence for  
948 liquid-liquid separation in supersaturated CaCO<sub>3</sub> solutions. *Science*, 341, 885-889.
- 949 Warren, B.E. (1990) X-ray Diffraction. Dover, New York.
- 950 Waychunas, G. A., Kim, C. S., and Banfield, J. F. (2005). Nanoparticulate iron oxide  
951 minerals in soils and sediments: Unique properties and contaminant scavenging  
952 mechanisms. *Journal of Nanoparticle Research*, 7, 409–433.
- 953 Waychunas, G. A., and Zhang, H. Z. (2008). Structure, chemistry, and properties of mineral  
954 nanoparticles. *Elements*, 4, 381–387.
- 955 Weber, F.-A., Voegelin, A., Kaegi, R. and Kretzschmar, R. (2009) Contaminant mobilization  
956 by metallic copper and metal sulphide colloids in flooded soil. *Nature Geoscience*, 2,  
957 267-271.
- 958 Williams, D.B., and Carter, C.B. (2009) Transmission electron microscopy. A textbook for  
959 Material Science (a four volume set). Springer.
- 960 Woehl, T.J., Jungjohann, K.L., Evans, J.E., Arslan, I, Ristenpart, W.D., Browning, N.D.  
961 (2013) Experimental procedures to mitigate electron induced artifacts during in situ  
962 fluid imaging of nanomaterials. *Ultramicroscopy*, 127, 53-63.
- 963 Wright, A.C. (1998) Diffraction studies of glass structure: The first 70 years. *Glass Physics*  
964 and Chemistry, 25, 148-179.

- 965 Yuan, G., and Wada, S.-I. (2012) Allophane and imogolite nanoparticles in soil and their  
966 environmental applications. In A.S. Barnard, and H. Guo, Eds., Nature's  
967 Nanostructures. Pan Stanford Publishing Pte. Ltd.
- 968 Yuk, J.M., Park, J., Ercius, P., Kim, K., Hellebusch, D.J., Crommie, M.F., Lee, J.Y., Zettl,  
969 A., Alivisatos, A.P. (2012) High-Resolution EM of colloidal nanocrystal growth  
970 using graphene liquid cells. *Science*, 336, 61-64.
- 971 Yuwono, V.M., Burrows, N.D., Soltis, J.A., and Penn, R.L. (2010) Oriented aggregation:  
972 Formation and transformation of mesocrystal intermediates revealed. *Journal of the*  
973 *American Chemical Society*, 132, 2163-2165.
- 974 Zhang, H., Gilbert, B., Huang, F., and Banfield, J.F. (2003) Water-driven structure  
975 transformation in nanoparticles at room temperature. *Nature*, 424, 1025-1029.
- 976 Zhu, M., Farrow, C.L., Post, J.E., Livi, K.J.T., Billinge, S.J.L., Ginder-Vogel, M., Sparks,  
977 D.L. (2012) Structural study of biotic and abiotic poorly-crystalline manganese  
978 oxides using pair distribution function analyses. *Geochimica et Cosmochimica Acta*,  
979 81, 39-55.

980

981

### FIGURE CAPTIONS

982 FIGURE 1A) Resolution limits of some common techniques used in the measurement of  
983 mineral crystallinity. The progressive fading from grey to white marks the lost of resolution  
984 of the different analytical techniques in the figure. The need of a multi-technique  
985 characterization to properly understand complex mineral phases is shown in the dashed  
986 extended area by the use of schwertmannite as a proxy for polyphasic nanominerals. B) Peak  
987 brilliance comparison between a selection of state-of-the-art 3<sup>rd</sup> generation synchrotrons and  
988 free electron lasers (FEL). Abbreviations: Advanced Light Source (ALS), Berliner  
989 Synchrotron (BESSY), Advance Photon Source (APS), European Synchrotron Radiation  
990 Facility (ESRF), Positron Electron Ring Angle (PETRA III), UE65 is part of PETRA, Super  
991 Photon Ring 8GeV (Spring-8), Free Electron Laser at Hamburg (FLASH), LINAC Coherent  
992 Light Source (LCLS), European XFEL operational in 2015 (XFEL). C) Evolution of  
993 Transmission Electron Microscopy (TEM) resolution. The graphic within the extended  
994 dashed area corresponds to the resolutions as a function of electron energy recently achieved  
995 by TEAM 0.5 project. Abbreviations: high vacuum (HV), high resolution (HR).



996

997       FIGURE 2. Schematic categorization of the natural progressive transition between  
998 amorphous and crystalline materials. The most relevant emerging areas within mineral  
999 crystallinity in environmental systems discussed in the main text have been exemplified with  
1000 some specific cases. The four categories shown within the mesocrystals inset correspond to  
1001 the alignment of nanoparticles by: a) organic matrices, b) physical fields and interparticles  
1002 forces, c) mineral bridges and d) space constrains.

# Fig. 1

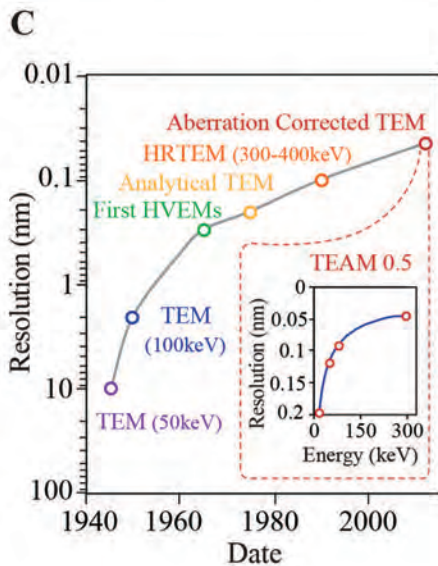
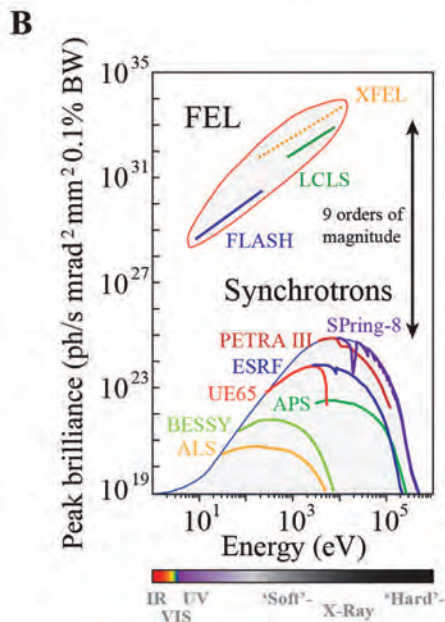
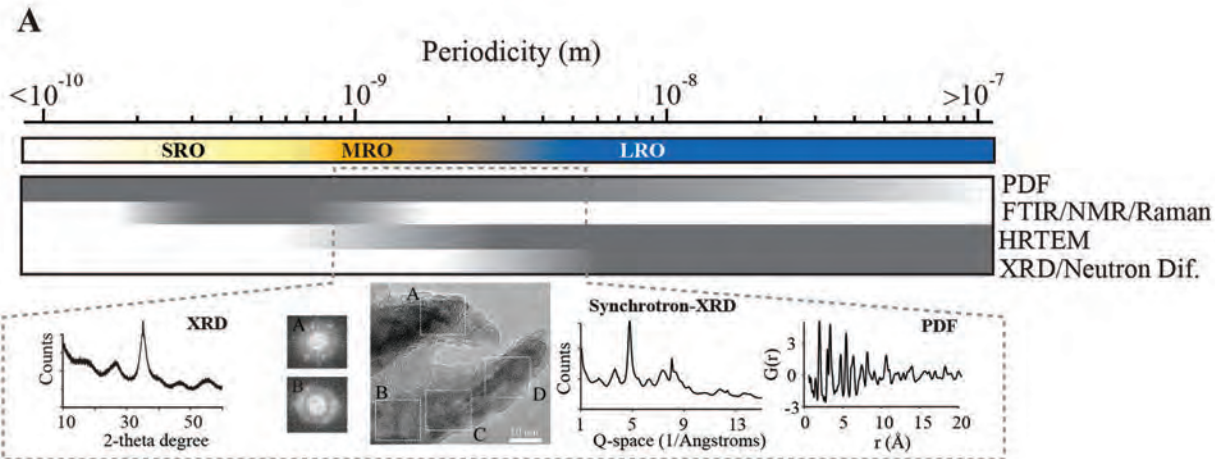


# Fig. 2

